Animal biology and pathology / Biologie et pathologie animales

Adrenal cortex disorders in a new model of obesity, *Gerbillus gerbillus*, exposed to a high carbohydrate diet

Désordres du cortex surrénalien chez un nouveau modèle d'obésité, Gerbillus gerbillus, soumis à un régime riche en hydrates de carbone

Maha Medjerab [a,*], Mohamed Abdelali [b], Ali Khalkhal [a], Nesrine Semiane [a], Soumia Hammadi [a], Aicha Mallek [a], Zineb Bellahrache [a], Hadjer Agoun [a], Yasmina Dahmani [a]

[a] LBPO/Nutrition–métabolisme, FSB/USTHB, BP 32, El Alia, 16111 Alger, Algeria
[b] Laboratoire de biologie cellulaire, CHU d'Hussein Dey, Alger, Algeria

ARTICLE INFO

ABSTRACT

Obesity is associated with several endocrine disorders, including hypersensitivity of the hypothalamic-pituitary-adrenal axis. The aim of this study was to investigate the effects of a high carbohydrate diet on structural and ultrastructural features of steroidogenic tissue, as well to evaluate adrenocorticotropic hormone (ACTH), cortisol, and insulin levels in the blood and steroidogenic acute regulatory protein (StAR) expression in the adrenals of gerbils. In electron microscopy, the most pronounced effect of the hypercaloric diet was observed in the *zona fasciculata*. Plasma levels of ACTH, cortisol, and insulin also showed significant increases. However, no significant change was noted in StAR protein levels. There is evidence that high carbohydrate intake brings about remarkable morphological and functional modifications. This could ultimately lead to mitochondrial alteration and accumulation of lipid droplets, which may lead to inflammation and degeneration of adrenal cells.

© 2019 Académie des sciences. Published by Elsevier Masson SAS. All rights reserved.

RÉSUMÉ

L'obésité est associée à plusieurs perturbations endocriniennes, y compris l'hypersensibilité de l'axe hypothalamo-hypophysaire surrénalien. Le but de la présente étude consiste à mettre en exergue les effets d'une alimentation riche en glucides sur les aspects structuraux et ultrastructuraux du tissu stéroïdien et d'évaluer les taux plasmatiques de l'ACTH, du cortisol et de l'insuline ainsi que les concentrations tissulaires surrénaliennes de la protéine StAR chez la gerbille. En microscopie électronique, les effets les plus prononcés du régime hypercalorique ont été observés dans la zone fasciculée. Des augmentations significatives des taux plasmatiques de l'ACTH, du cortisol et de l'insuline ont été enregistrées ; cependant, aucun changement significatif n'a été noté concernant les concentrations en protéines StAR. Le régime hypercalorique induit dans le tissu stéroïdien

---

* Corresponding author.
  E-mail address: medjerab.maha@gmail.com (M. Medjerab).

des modifications morphologiques et fonctionnelles remarquables, qui peuvent résulter d'une forte accumulation lipidique et d'une altération mitochondriale pouvant conduire à un état inflammatoire et à une dégénérescence cellulaire.

1. Introduction

Obesity in humans has become a major public health concern and has reached epidemic proportions worldwide [1]. In basic terms, it results from the perturbation of energy equilibrium by consuming more energy than is spent, resulting in fat production and storage [2]. It is widely accepted that dietary and lifestyle factors are the primary causes of obesity and its related problems [2]. The pathogenesis of obesity is frequently associated with several metabolic and endocrine disorders, leading to serious complications, such as type-2 diabetes mellitus and cardiovascular diseases [1]. It is also strongly associated with hyperactivity of the hypothalamus-pituitary-adrenal (HPA) axis [3,4].

Hyperactivity of the HPA axis has an effect on the body's stress response in the sense that an excess of glucocorticoids is secreted by the adrenal gland [5,6]. Because of the crucial role of adrenal function in the body's homeostasis, adrenal dysfunction is an important factor in the development of obesity related abnormalities [7]. Adrenal dysfunction is an important factor in the pathogenesis of obesity due in part to the similarities between metabolic abnormalities in central obesity and glucocorticoids excess secretion.

Steroid hormone synthesis is controlled by the activity of several highly substrate-selective cytochrome p450 enzymes (CYPs) and a number of steroid dehydrogenases (HSDs) and reductases. The biosynthesis of adrenal steroids is primarily activated through stimulation by trophic hormones and involves the activation of adenylate-cyclase activity, which results in increased cAMP levels and protein kinase A (PKA) activation [8]. Signals that stem from trophic hormone stimulation increase cholesterol transport to the cytochrome P450 side-chain cleavage (P450scc) enzyme, which resides on the inner mitochondrial membrane. Cholesterol transport is mediated by transport proteins, primarily steroidogenic acute regulatory protein (StAR) [9]. StAR protein is a component of a protein complex that functions in the rate-limiting step of steroidogenesis [10,11]. The crucial role of StAR in the regulation of steroidogenesis was discovered by treating patients suffering from lipoid congenital adrenal hyperplasia (lipoid CAH), an autosomal recessive disorder in which both adrenal and gonadal steroid biosynthesis is severely impaired owing to mutations in the *StAR* gene [12]. The targeted disruption of the *StAR* gene in mice resulted in a phenotype essentially identical to that found in lipoid CAH in humans [13].

Mitochondria are central in steroidogenesis since the physical protein–protein interactions between key factors during the transport of cholesterol take place in the contact sites between the two mitochondrial membranes, thus suggesting that mitochondrial integrity might potentially limit this process.

This study aims to define the relationship between the functional status and ultrastructural features of the adrenal gland in a new model of obesity, *Gerbillus gerbillus*.

2. Materials and methods

2.1. Animal and experimental design

G. gerbillus individuals were collected from the semi-desert region of Beni-Abbes (900 km southwest of Algiers). The authorization to capture the animals in desert region was given by the Ministry of Higher Education (Algeria). The average weight of adult male and female gerbils used was between twenty-two and twenty-four grams. They were housed in individual cages under controlled light/dark cycle (12 h/12 h) and maintained under controlled temperature (23 ± 2 °C) conditions. All animals received a low carbohydrate diet composed of lettuce, carrots, and other succulent parts of plants (*Zygophyllum album*) ad libitum.

After two weeks of adaptation, gerbils of both sexes were divided into two groups and weighed (Table 1 gives data for the average initial values of the body weight taken after two weeks of adaptation). The first group ($n = 12$) served as controls, maintained on the same low carbohydrate diet, corresponding to a daily calorific intake of 10 kCal/animal. The second group ($n = 12$) was the experimental one, which received a high carbohydrate diet, consisting exclusively of barley and dry dates *ad libitum*, corresponding to a daily calorific intake of 22.5 kCal/animal.

Blood samples from individual gerbils were collected after two weeks of adaptation by puncture from the retro-orbital venous plexus in separate tubes containing the anticoagulant EDTA. Plasma was separated though centrifugation at 3000 *g* for 10 min, for later ACTH, cortisol, and insulin estimations, corresponding to the initial concentrations (Table 2). In order to avoid the influence of nycthemere, blood punctures were practiced in the morning consistently fasted for between 08:00 and 10:00 on all animals.

After six months on the diet, gerbils of both groups were weighed (Table 1 gives data for the average final values of the body weight) and then sacrificed by decapitation in the morning (between 09:00 and 12:00). The blood was collected into 0.1 mM EDTA-treated plastic tubes on ice, centrifuged at 3000 *g* for 10 min and plasma stored at –20 °C for later ACTH, cortisol, and insulin determinations, corresponding to the final concentrations (Table 2). All adrenal glands were removed, rinsed with cold 0.9% NaCl

Table 1
Body and adrenal gland weights.

Treatment group	Body weight (g)		Relative adrenal gland weight (mg)	
	Initial weight	Final weight	Left adrenal	Right adrenal
Control (n = 12) Low carbohydrate diet ≈ 10 kCal/day	22.82 ± 0.52	22.71 ± 1.25[a]	22.59 ± 2.55	20.52 ± 1.79
Experimental (n = 12) High carbohydrate diet ≈ 22,5kCal/day	22.70 ± 0.49	33.25 ± 0.75[b,e]	32.06 ± 2.05[d]	25.98 ± 1.54[c]
% Increases		46.41	41.92	26.6

Data are expressed as means ± SEM.
[a] Initial body weight *vs* final body weight, $P > 0.05$.
[b] Initial body weight *vs* final body weight, $P < 0.0001$.
[c] Experimental *vs* control., $P < 0.05$.
[d] Experimental *vs* control., $P < 0.01$.
[e] Experimental *vs* control., $P < 0.0001$.

Table 2
Plasma levels of ACTH, cortisol and insulin in the control and experimental groups.

Plasma levels	Initial values (n = 6)	Control (n = 6)	Experimental (n = 6)	% Increase (experimental *vs* control)
ACTH (pg/mL)	1541.48 ± 234.16	1704.60 ± 380.42[a]	2890.68 ± 413.45[b,d]	69.58
Cortisol (nmol/L)	215.73 ± 34.89	224.04 ± 39.58[a]	404.02 ± 60.43[b,e]	80.33
Insuline (μUI/mL)	37.28 ± 10.80	37.62 ± 8.63[a]	113.32 ± 11.12[c,f]	201.22

Data are expressed as means ± SEM.
[a] Initial values *vs* control, $P > 0.05$.
[b] Experimental *vs* initial values, $P < 0.01$.
[c] Experimental *vs* initial values, $P < 0.001$.
[d] Experimental *vs* control, $P < 0.05$.
[e] Experimental *vs* control, $P < 0.01$.
[f] Experimental *vs* control, $P < 0.001$.

and weighed. Six adrenals right and left, of each group, were frozen at –80 °C for StAR protein analysis until use, others six right adrenals cutting in half, were fixed into 10% formalin solution for light microscopy examination, whereas the corresponding left adrenals were immersed in a mixture of 2.5% glutaraldehyde-4% paraformaldehyde diluted in 0.1 M phosphate buffer for electron microscopy.

2.2. Hormone assays

ACTH levels in 200-μL samples of plasma were measured by immunoradiometric assay (ELSA-ACTH Kit; Cisbio Bio Assays, France), using two monoclonal anti-ACTH antibodies. The first antibody specific for the N-terminal part of ACTH was coated onto the ELSA solid phase, and the second antibody specific for the C-terminal part of ACTH was radiolabelled with ^{125}I. The radioactivity bound to the ELSA is proportional to the concentration of ACTH present in the sample. The detection limit for ACTH was determined to be 2 pg/mL ($7.3 \cdot 10^{-12}$ mol/L).

Cortisol and insulin levels in 20-μL and 100-μL aliquots of plasma were measured using a competitive binding method according to the protocol supplied with the kits (Cisbio Bio Assays, France).

The detection limit for insulin was 4.6 μIU/mL ($3.19 \cdot 10^{-11}$ mol/L), and 6.6 nmol/L ($6.6 \cdot 10^{-9}$ mol/L) for cortisol. The cortisol antiserum showed a 2.5% cross-reactivity with corticosterone.

2.3. Light and electron microscopy

2.3.1. Sample preparation

The adrenal glands of each group of gerbils were stripped of surrounding fat tissue, without injuring the capsule, cut in halves and immersed both in 10% formalin during 48 h for histological examination. After routine processing, dehydration in graded ethanol, and soaking in paraffin, each paraffin block was cut into 5-μm-thick slices using a microtome (Leica, Germany), stained with Masson's trichrome, and observed with a Zeiss photonic microscope.

For ultrastructural studies, small pieces of the adrenal glands were fixed in a mixture of 2.5% glutaraldehyde-4% paraformaldehyde diluted in 0.1 M phosphate buffer at pH 7.4 for 2 h at 4 °C, the pieces were then rinsed in 0.2 M phosphate buffer, then post-fixed in 1% solution of osmium tetroxide (1% OsO$_4$) during 1 h at 4 °C, dehydrated in ethanol, cleared in propylene oxide, embedded in Epon 812 resin and polymerized. Ultrathin sections were cut with an ultra-microtome, stained with solutions of uranyl acetate and lead citrate, and examined with a *Hitachi HT7700* transmission electron *microscope* (Delta Microscopies, France).

2.4. Western blot

Whole-cell protein extracts were obtained from adrenal samples by homogenizing in Laemmli buffer [14] using an

ultrasound homogenizer and centrifuging for 25 min at 14,000 *g* at 4 °C. The proteins were quantified by the Bradford method [15]. Denatured protein extracts (15 μg) were resolved on 10% sodium dodecyl sulfate-polyacrylamide gel (SDS–PAGE) and electrophoresis according to the method of Laemmli [14]. The proteins were transferred onto polyvinylidene difluoride (PVDF) membranes (0.45 μm) using a transfer buffer (25 mM Tris, 192 mM glycine, and 20% methanol) at 100 V for 1.5 h at 4 °C. After that, the membranes were blocked with tris-buffered saline (TBS-T: 50 mM Tris–HCl, pH 8, 150 mM NaCl and 0.3% (v/v) Tween 20) containing 5% (w:v) non-fat dry milk for 1 h at room temperature to reduce non-specific protein-binding, and then they were probed with an appropriate dilution of primary antibody overnight at 4 °C. The antibody used was a rabbit polyclonal anti-StAR (1:1000, a kind gift from Dr D.M Stocco, Tech University Health Sciences Center, TX, USA). After extensive washing (TBS 0.3% Tween 20), membranes were incubated with secondary antibody (1:1000, a kind gift from Dr E. Lalli, "Institut de pharmacologie moléculaire et cellulaire", Nice) for 1 h at room temperature.

The normalization of the bands was performed by reprobing the membranes with beta-actin antibody after washing with a tris-buffered saline solution (TBS 0.3% (v/v) Tween 20) and by blocking with TBS-T 0.3% (v/v) Tween 20 containing 5% (w:v) of non-fat dry milk. Immunoreactive proteins were visualized using the enhanced chemiluminescence kit, and the images were captured using a chemiluminescence imaging system (IPMC, CNRS, Nice). The acquired protein bands appeared white against a dark background due to the light emitted by the oxidation of luminol. The immunoreactive bands were evaluated by measuring the area and its density with Image J software (IPMC, CNRS, Nice).

2.5. Statistical analysis

Data are expressed as means ± SEM (standard error of the mean). Differences in means between two groups of gerbils were determined with Student's *t* test. The differences are considered significant at $P < 0.05$.

3. Results

3.1. Changes in body, adrenal weights and hormonal levels

As shown in Table 1, the high carbohydrate diet resulted in significant increases in the final body and adrenals relative weights compared to the control group. The increase was about 46.41% ($P < 0.0001$) for body weight, 26.6% ($P < 0.05$) for right adrenals, and 41.92% ($P < 0.01$) for left adrenals. Elevated ACTH (by 69.58%), cortisol (by 80.33%), and insulin (by 210.22%) levels in plasma were observed in the experimental group as compared to the control group (Table 2); these changes were statistically significant and corresponded to $P < 0.05$, $P < 0.01$, and $P < 0.001$, respectively.

In contrast, the control animals exhibited no significant change in body weight and ACTH, cortisol and insulin
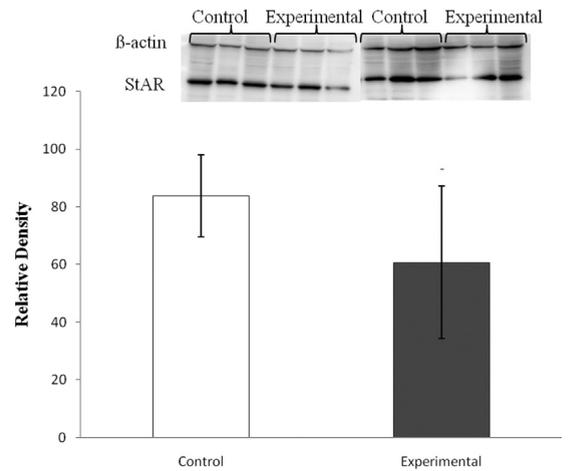
Fig. 1. StAR relative density normalized to β-actin in adrenal glands of *Gerbillus gerbillus* under low and high carbohydrate diets. (Experimental *vs* control, $P > 0.05$).

plasma levels ($P > 0.05$) compared to the initial values and were recovered at a similar rate.

3.2. Expression of StAR protein in adrenal extracts

An immunoreactive signal corresponding to StAR protein (30 kDa) was detected in adrenal extracts from both groups. The high carbohydrate diet tended to decrease the protein level of StAR as compared to control diet-fed gerbils, but the decrease was not significant ($P > 0.05$) (Fig. 1).

3.3. Histological and ultrastructural examination

3.3.1. Control animals
Representative photomicrographs of the control adrenal sections are presented in Fig. 2.

Adrenal sections of control animals showed a normal adrenal architecture. The parenchymal cells of the cortex between the capsule and medulla revealed three different types of arrangements. In the *zona glomerulosa* (Fig. 2, **A**.a, B.a,b,c), the cells were grouped into small, irregular clusters (Fig. 2, **A**.a), surrounded by a network of fenestrated capillaries (Fig. 2, **B**.a). Their nuclei were somewhat smaller and darker than those of the next zone (Fig. 2, **A**.a) and showed a nucleolus. Likewise, their cytoplasm was of a more even texture, but contained some lipid droplets varying greatly in size (Fig. 2, **B**.a,b). Some of these lipid droplets appeared to be confluent (Fig. 2, **B**.b). Beneath this was a thick layer, the *zona fasciculata* (Fig. 2, **A**.b, **B**.d,e,f), in which the cells were roughly polyhedral, and had distinct cell membranes with reduced intercellular spaces (Fig. 2, **B**.d,e). They were arranged in cords (Fig. 2, **A**.b, **B**.d) perpendicular to the capsule, with straight capillaries between them. Their nuclei were larger and less dense than those of the *zona glomerulosa*. The cytoplasm appeared to be extensively vacuolated. These are referred to as spongiocytes (Fig. 2, **A**.b, **B**.d,e) because they contain large numbers of lipid droplets (cholesterol esters, which are precursors of steroid
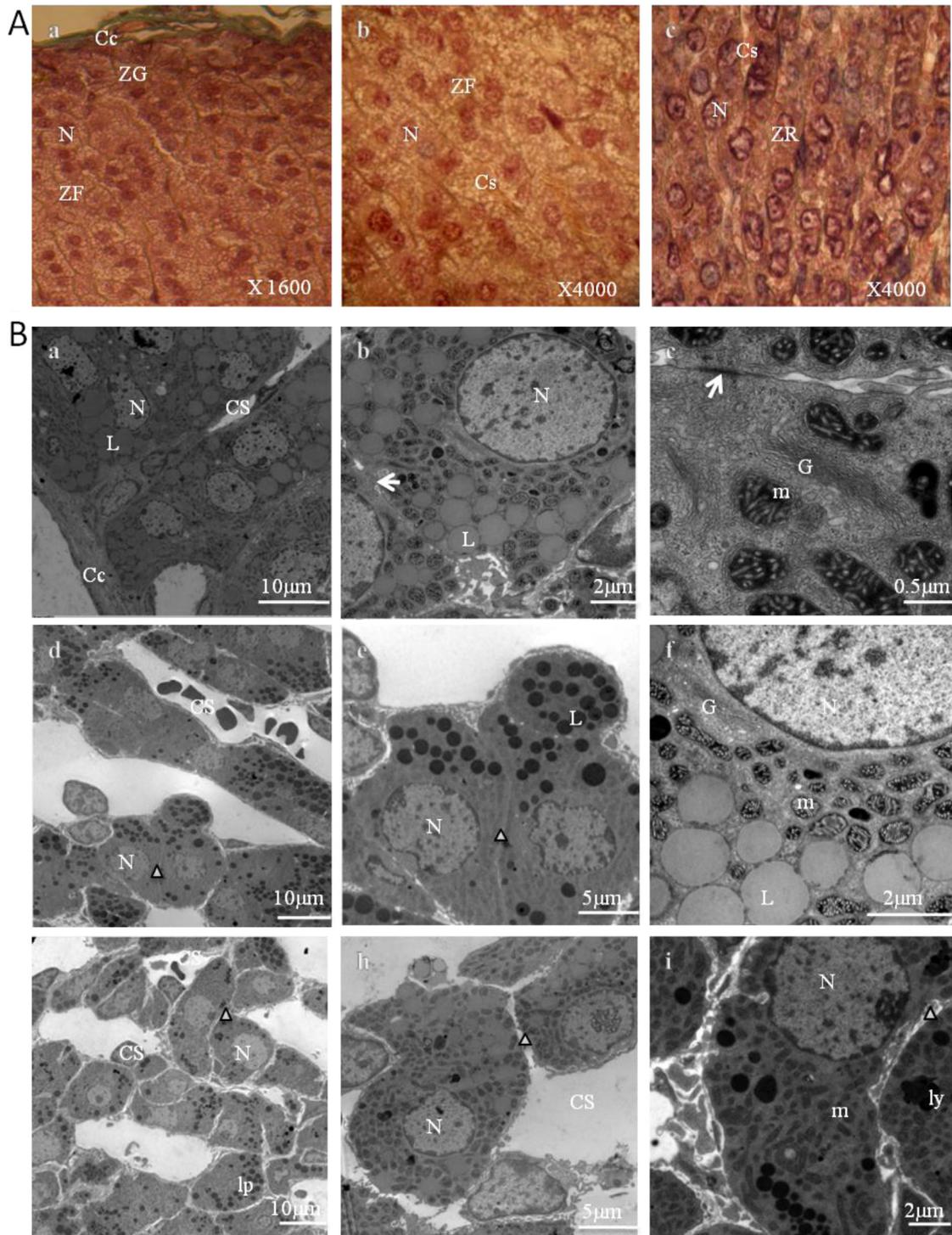
Fig. 2. Adrenal cortex of control gerbils. A. Histological findings (stained with Masson's trichrome). ZG: *zona glomerulosa* (a); ZF: *zona fasciculata* (b); ZR: *zona reticularis* (c); Cc: conjunctive capsule; N: nucleus; Cs: blood capillaries. B. Ultrastructural aspects of a portion of the *zona glomerulosa* (a–c), *zona fasciculata* (d–f), and *zona reticularis* (g–i). Cc: capsular; N: nucleus; Cs: blood capillaries; L: lipid droplet; (arrow): gap junction; G: Golgi apparatus; m: mitochondria; cv: coated vesicles; Δ: intercellular space; ly: lysosomes; lp: lipofuscins.

hormones). The cells were rich in mitochondria, located very close to the lipid droplets, and marked by a dark mitochondrial matrix and tubular cristae (Fig. 2, **B**.f).

The cells of both the *zona glomerulosa* and *zona fasciculata* contained large amounts of smooth endoplasmic reticulum. They also contained a few lysosomes.

In the *zona reticularis* (Fig. 2, **A**.c, **B**.g,h,i), cells were positioned in cords that run in various directions and anastomosed with one another (Fig. 2, **A**.c, **B**.g). Some cells have a small dark nucleus and acidophilic cytoplasm, and relatively low lipid content. Others had a lighter nucleus and cytoplasm (Fig. 2, **A**.c). Some cells contained considerable quantities of lipofuscin pigment. Like the cells in the two other zones, they contained abundant amounts of smooth endoplasmic reticulum.

3.3.2. Animals fed a high carbohydrate diet

These adrenal glands showed striking differences in structural and ultrastructural features compared to the control adrenal glands. These findings are depicted in Fig. 3.

The adrenal cortex showed a cellular hypertrophy, which was more marked in the *zona fasciculate* (Fig. 3. 2**A**.b,c). In this zone, the cellular arrangement of the few cell cords was irregular (Fig. 3, 2**A**.b,d,e) and the extracellular spaces between these cell cords were large (Fig. 3, 2**A**.d, 2**B**.d,e). Sometimes the venous sinuses were dilated (Fig. 3, 2**A**.d, 2**B**.d,e), and the endothelial cells were dissociated from the basal lamina. The presence of adipose tissue in some areas was also noted, most of all in the *zona fasciculata* (Fig. 3, 2**A**.e). We have also noted a loss of *zona glomerulosa* in some areas in the experimental glands (Fig. 3, 2**A**.a).

Moreover, the cells in the three zones (*glomerulosa, fasciculata,* and *reticularis*) were surrounded by a blurred plasmatic membrane (Fig. 3, 2**B**.a,i,k,q) and they were in particular characterized by a largely developed smooth endoplasmic reticulum and a Golgi apparatus. Numerous lysosomes with high electron density were also observed (Fig. 3, 2**B**.e,f,g,h,i,l,o,p).

An increase in the number of mitochondria and lipid droplets was also noted (Fig. 3, 2**B**.c,i,j,k,l,q). This was most evident in the *zona fasciculata.*

Mitochondria were abundant, scattered throughout the cytoplasm, their crests were dilated, and their matrices were finely granular and less dense to electrons (Fig. 3, 2**B**.i,l,r).

The lipid droplets were variable in size and shape and more numerous than those observed in the cells of the control adrenal glands, especially in the *zona fasciculata.* Sometimes, they were scant and appeared in connection with mitochondria and smooth endoplasmic reticulum. Their close association suggests the active biosynthesis of steroid hormones. Sometimes they appeared to be surrounded by membrane, fusing with autophagic vesicles (Fig. 3, 2**B**.c,i,l).

Large focal areas of mature fibrous connective tissue in the *zona fasciculata* (Fig. 3, 2**B**.f,j) and the *zona reticularis* (Fig. 3, 2**A**.f, 2**B**.n,o) were observed, and there were scattered fibroblasts and blood vessels within the fibrotic areas.

The cells were sometimes connected by tight junctions (Fig. 3, 2**B**.b,r). In the cytoplasm, one could also observe lamellar formations, dense bodies, multivesicular bodies and coated vesicles, some of which were associated with the lamellae of the Golgi apparatus. Tubular profiles of smooth endoplasmic reticulum were observed scattered in
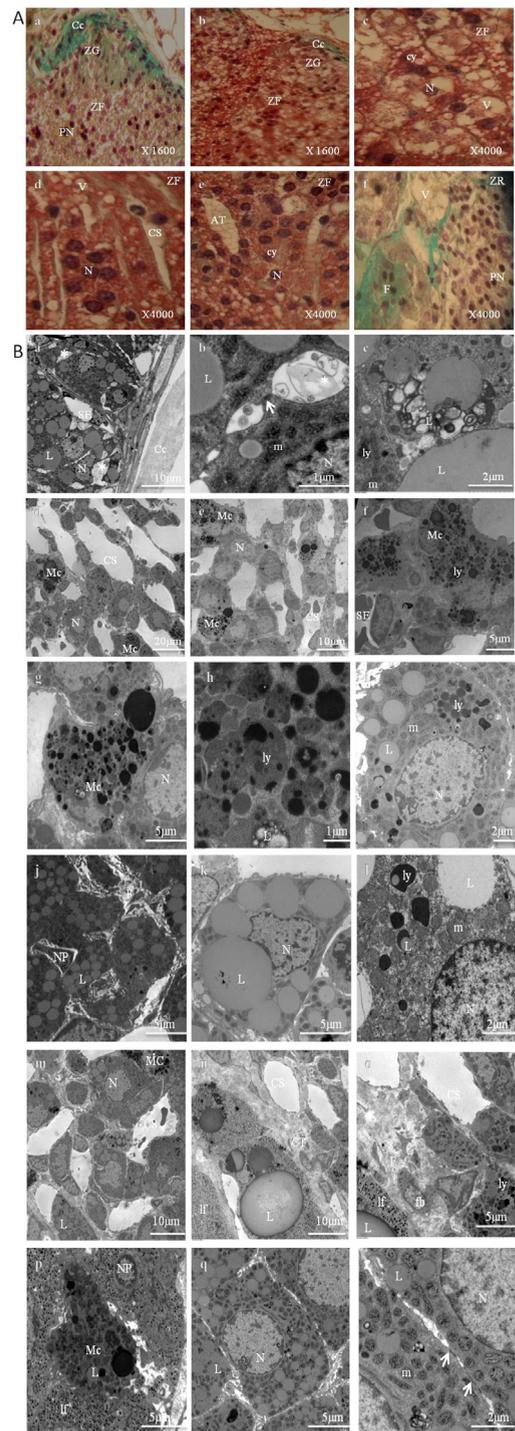
Fig. 3. Adrenal cortex of gerbils fed a high carbohydrate diet. 2A. Histological findings (stained with Masson's trichrome). ZG: *zona glomerulosa* (a and b); ZF: *zona fasciculata* (c–e); ZR: *zona reticularis* (f); Cc: conjunctive capsule; cy: cytoplasm; N: nucleus; PN: pyknotic nuclei; Cs: Blood Capillaries; V: vacuolizations; AT: adipose tissue; F: fibrosis. 2B. Ultrastructural aspects of a portion of the *zona glomerulosa* (a–c), *zona fasciculata* (d–l), and *zona reticularis* (m–r). Cc: capsular; N: nucleus; Cs: dilated blood capillaries; L: lipid droplet; (arrow): gap junction; G: Golgi apparatus; m: spherical mitochondria with atypical crests and a less dense matrix; *: dilated intercellular space; ly: lysosomes; lp: lipofuscins; SE: sinusoid endothelium; F: fibrosis; PN: pycnotic nucleus; CT: conjunctive tissue; fb: fibroblast; Mc: macrophage.

the cytoplasm. Some cells degenerated, their residues could be seen in intercellular spaces (Fig. 3, 2**B**.b,r). They were phagocytized by macrophages, which create a widening in the intercellular spaces. The number of macrophages was markedly increased in the *zone fasciculata* (Fig. 3, 2**B**.d,e,f) and *reticularis* (Fig. 3, 2**B**.m,p). Numerous lipid droplets and lysosomes were observed in each macrophage and those with heterogeneous matrixes were larger and their content more complex. These results show that a high carbohydrate diet stimulates the adrenal macrophage system, which causes an inflammatory state.

4. Discussion

Gerbils (*G. gerbillus*) as an animal model display several correlations with human obesity. In this study, it was shown that high carbohydrate feeding for six months induced obesity as well as endocrine perturbations and elicited remarkable morphological changes in the adrenal cortex.

Hyper-calorific diets have been linked to a positive energy balance, weight gain, obesity, and metabolic syndrome [16]. In *G. gerbillus*, the increase in energy intake by the overconsumption of simple sugars contained in dry dates, mainly glucose and fructose, resulted in a positive energy balance with cumulative effects over the six-month study period. This resulted in marked increases in body weight (about 46.41%), with an accumulation in visceral adipose tissue and ectopic fat deposits. This latter result fits well with data showing an increased de novo lipogenesis in humans after long-term fructose feeding [17], as well as in high carbohydrate diet in gerbils [18]. This is the first report showing an ectopic accumulation of lipids in the adrenal cortex of gerbils fed a high carbohydrate diet. In humans, in peripheral tissue, increased flux of energy fuel substrates associated with high-fat or high-sucrose diets leads to ectopic lipid accumulation, generation of reactive oxygen species (ROS), and cellular dysfunction, a phenomenon known as glucolipotoxicity [19].

This high carbohydrate diet also caused a significant increment in the plasma insulin level (by 210.22%). In accordance, increased fructose intake has demonstrated to induce hyperinsulinemia and insulin resistance in humans [20], rats [21], and gerbils [18]. The experimental gerbils also displayed a hyperactive hypothalamic–pituitary–adrenal (HPA) axis, as stated before, with elevated plasma ACTH (+69.58%) and cortisol (+80.33%). A major neuroendocrine mechanism in a stress reaction is the activation of the hypothalamic–pituitary–adrenal (HPA) axis, resulting in a rapid increase in circulating corticotrophin (ACTH) and subsequent rise in glucocorticoids, which are critical for successful adaptation [22]. Thus, plasma levels of ACTH and glucocorticoids are a good indicator of stress response intensity, particularly in its acute phase [23]. All these processes are adaptive, designed to re-establish homeostasis, but it is also apparent that prolonged activation of stress systems can disturb normal physiological and behavioral function. Our results fit well with data showing a dysregulation of the hypothalamic–pituitary–adrenal (HPA) axis, resulting in a higher ACTH output leading to elevations in glucocorticoids in diet-induced obesity [24] and in obese humans displaying features of insulin resistance [25]. It is interesting to note that, after six months of dietary treatment, the experimental group exhibited no significant changes in StAR protein levels in adrenal extracts, a key protein involved in the early steps of steroidogenesis. StAR activity is a major determinant of the levels of circulating glucocorticoids, which the body uses to respond to both diet and stress [26]. Our results prompt us to propose the involvement of effectors other than StAR protein in the genesis of basal hypercorticosteronemia. Increased levels of fatty acids or other lipid metabolites, within the adrenal cortex, could be involved in the dysregulation of basal corticosterone production [27]. The regulation of steroidogenesis by adipocyte secretory products, generated by fat cells, present in close contact with steroidogenic cells, has also been shown [28], and evidence of cytokines originated within the adrenal tissue must also be considered [29]. Importantly, our electron microscopic examination showed a macrophage infiltration in the adrenal cortex.

Our findings indicate that adrenal cortical function is directly affected by high-carbohydrate diet in gerbils. We proposed that, through dysregulation of glucocorticoid signaling, a high carbohydrate diet may better predict the promotion and maintenance of obesity and hyperinsulinemia in gerbils. The fact that there are very few reports on a morphological analysis of adrenal glands after high carbohydrate diet feeding, we decided to determine the effect of the diet on gerbils' adrenal gland morphology.

In the current study, the histological and cytological observations correlate perfectly with the endocrine perturbations. The morphology of the adrenal glands of the experimentally studied gerbils changes in response to the high-carbohydrate diet. All three cortical zones are affected, the *zona fasciculata* is typically the most severely affected, although eventually the lesions involve the *zona glomerulosa* and the *zona reticularis*. The changes are caused by the increased circulating levels of ACTH, which caused an increase in the width of the *zona fasciculata*, with an increase in cell size, resulting in a significant increase in adrenal relative weight (+26.6% for right adrenals and +41.92% for left adrenals). The adrenocortical hypertrophy, a common finding in toxicology studies, may readily be induced in the rat by ACTH treatment [30]. This is also reported in mice fed a high-fat diet [31] and connected to several types of stress [32]. In accordance with Nussdorfer [33], the trophic effect of ACTH evokes an increase in adrenal mass and in the steroidogenic capacity of adrenocortical cells [33]. The increased circulating levels of ACTH also have a profound effect on the adrenal vasculature of experimental gerbils, causing a marked vasodilation in the *zona fasciculate*, which led to the gross distortion of the organization and disruption of the cord-like arrangement of this zone. This is described in rat adrenal glands under chronic ACTH treatment [34]. Sricharoenvej et al. [35] reported that the luminal diameters of capillaries were dilated in all zones in adrenal glands in diabetic rats. Kanczkowski et al. [36] proposed that endothelial dysfunction might participate in inflammation-related adrenal insufficiency.

We have also noted a loss of *zona glomerulosa* in some areas in the experimental glands, with the transformation of the *glomerulosa* cells into *fasciculate*-type cells. This is also observed in the adrenal cortex of the rat under ACTH treatment and, at the same time, a loss of aldosterone synthetic capacity is observed [34]. There are some reports suggesting that the *zona glomerulosa* could be the source of new cortical cells [37].

In gerbils fed a high carbohydrate diet, the adrenal cells become constantly stimulated and are hyperactivated up to alteration. This is believed to reflect a difference in the degree of stress in cells and in the release of ACTH and glucocorticoids. Adrenal cells of experimental gerbils, most of all, in *zona fasciculata* and in *zona reticularis*, appeared altered and exhibited other ultrastructural changes compared to the control group.

The most striking structural change consists of a marked accumulation of lipid droplets in focal cytoplasmic areas and of a notable decrease in the electron density of the mitochondrial matrix. Pycnosis, vacuolisation, fibrosis, and macrophage infiltration were also observed. Our present report corroborates the finding in the sand rats (*Psammomys obesus)* when submitted to nutritional stress [38]. The vacuolisation and pycnosis, are common abnormalities due to acute injury, fibrosis, and hyperplasia seem to be chronic repair processes [39].

The finding of dilated pericapillary spaces and blurred plasma membranes in glands of experimental gerbils suggests a compensatory change to increase HDL (high density lipoprotein) and/or LDL (low density lipoprotein) uptake, as observed under ACTH stimulation [40]. In the experimental group, the cells of *zona fasciculata* showed a dilated smooth endoplasmic reticulum. According to some investigators, smooth endoplasmic reticulum is also involved in the endogenous synthesis of cholesterol from acetate [41]. Since cholesterol esters are the most important components of the lipid droplets [42], it is conceivable that the hypertrophy of the smooth endoplasmic reticulum would enable *zona fasciculata* cells to store as lipid droplets increased amounts of corticosterone precursors (cholesterol esters).

Sometimes, the lipid droplets in adrenal glands of experimental gerbils appeared sequestered in autophagosomes, which fused with lysosomes. A bidirectional interrelationship exists between autophagy and lipid stores, as increased cellular lipid content decreases autophagic function [43]. Autophagy therefore represents a new cellular target for abnormalities in lipid metabolism and accumulation [44]. By measuring autophagic vacuole fractional volume in adrenocortical *zona fasciculata* cells in rats exposed to adrenocorticotropic hormone (ACTH), Müller et al. [45], showed that autophagy was strongly inhibited during ACTH-induced hyperplasia.

Most importantly, adrenal glands of experimental gerbils displayed mitochondrial abnormalities. Mitochondrial cristae were dilated and impaired. A similar finding was observed in adrenal mitochondria of sand rats when submitted to nutritional stress [38]. Mitochondria modify their distribution, structure, and function in response to changing circumstances such as stress [46]. Adrenal mitochondria of experimental gerbils also showed a loss of matrix density compared to the control group. Several authors have described possible diet-induced changes in mitochondrial respiratory chain activity and respiration.

In hepatic mitochondria of rats, the cytochrome oxidase activity has been found increased [47], reduced [49] in response to a high fat feeding and unchanged in obese Zucker rats [48]. Similar findings on the loss of matrix density were observed in hepatic mitochondria of mice fed a high-fat diet [50], in oxidative stress conditions [51] and in response to ageing [52] in human cells. Excess in energy intake and/or a high degree of mitochondrial coupling cause(s) an increase in proton motive force to a maximum, with respiratory complexes that become highly reduced and may release electrons directly to oxygen, resulting in a higher ROS production. The mitochondrial dysfunction could be an important determinant of the cellular fate of circulating lipids that accumulate in the cytoplasm if they are not oxidized. Excessive energy substrates lead to mitochondrial dysfunction and abnormal lipid metabolism, which may be related to chronic low-grade-inflammation.

An additional finding of interest was the presence of an inflammatory process in adrenal glands of experimental gerbils. Both macrophages infiltration and fibrosis were present in the *zona fasciculata* and the *zona reticularis* in adrenals of experimentally studied gerbils. Similar, Omari et al. [38] reported that a high carbohydrate diet induces fibrotic programs, with infiltrating macrophages in adrenal glands of obese sand rats [38]. Experimental data support causative roles for hyperglycemia in alterations in collagen-rich extracellular matrix (ECM) turn-over [53]. One class of molecules that are thought to be important in the maintenance of the ECM and processes of tissue repair are matrix metalloproteinases (MMPs). The MMPs are primarily responsible for the turnover and degradation of ECM. In our experiment, this balance was upset, resulting in increased synthesis, decreased degradation, or a combination of perturbations to both processes, resulting in progressive deposition of ECM in adrenal glands. In agreement, Reichenstein et al. [54] suggest that ACTH may modulate the activities of MMPs, and hence cell matrix remodelling [54]. Many of the studies on the effects of glucocorticoids on the expression of MMPs have addressed pathological conditions. Some studies support that glucocorticoids can down-regulate the expression of several MMPs [55]. Further studies are necessary to conclude in favor of a causal association between the activity of the HPA and the levels of MMPs.

Degenerative signs were also observed in the adrenal cells of experimentally studied gerbils. Our examination showed a pycnosis (nuclear condensation), vacuolization, and the presence of a substantial amount of edema in the intercellular spaces. These findings correspond with the initial post-mortem autolytic changes reported in previous studies, in kidney, pancreas, liver, heart and skeletal muscle of rats [56]. The mechanisms inducing cell death in the adrenal glands are present, and they serve to control cell proliferation and perhaps functional cell hyperactivity.

Taken together, the finding of degenerative cellular and prominent infiltration of macrophages, with cytoplasmic lipid droplets observed in the stromal macrophages,

suggests that intracellular lipid accumulation becomes toxic for steroidogenic cells. We propose a paracrine interaction between adrenocortical cells and macrophages. This immune-endocrine cross-talk becomes evident in the case of autoimmune and inflammatory diseases, being necessary for an adequate adrenal stress response. The inflammatory and apoptotic markers suggest a new way of analysing the gland under stress.

Our results support the emerging idea that adrenal mitochondrial dysfunction in obesity is closely related to perturbation in lipid metabolism, which could result in lipotoxicity in adrenal cells.

5. Conclusion

There is a defective adrenal cortex activity associated with obesity and a possible link between adrenal mitochondrial dysfunction and diet-induced obesity. This direct effect of diet on adrenal steroidogenesis should have important physiological and/or pathophysiological significance, including inflammation and apoptosis, and deserves further investigations.

References

[1] B. Caballero, The global epidemic of obesity: an overview, Epidemiol. Rev. 29 (2007) 1–5.
[2] A. Tremblay, L. Pérusse, C. Bouchard, Energy balance and body-weight stability: impact of gene-environment interactions, Br. J. Nutr. 92 (2004) 63–66.
[3] R. Pasquali, V. Vicennati, M. Cacciari, U. Pagotto, The hypothalamic-pituitary-adrenal axis activity in obesity and the metabolic syndrome, Ann. N.Y. Acad. Sci. 1083 (2006) 111–128.
[4] D.J. Wake, B.R. Walker, 11beta-hydroxysteroid dehydrogenase type1 in obesity and the metabolic syndrome, Mol. Cell. Endocrinol. 215 (2004) 45–54.
[5] J.J. Haddad, N.E. Saadé, B. Safieh-Garabedian, Cytokines and neuro-immune-endocrine interactions: a role for the hypothalamic-pituitary-adrenal revolving axis, J. Neuroimmunol. 133 (2002) 1–19.
[6] H.C. Atkinson, S.A. Wood, Y.M. Kershaw, E. Bate, S.L. Lightman, Diurnal variation in the responsiveness of the hypothalamic-pituitary-adrenal axis of the male rat to noise stress, J. Neuroendocrinol. 18 (2006) 526–533.
[7] V. Lamounier-Zepter, M. Ehrhart-Bornstein, Fat tissue metabolism and adrenal steroid secretion, Curr. Hypertens. Rep. 8 (2006) 30–34.
[8] D.M. Stocco, X. Wang, Y. Jo, P.R. Manna, Multiple signaling pathways regulating steroidogenesis and steroidogenic acute regulatory protein expression: more complicated than we thought, Mol. Endocrinol. 19 (2005) 2647–2659.
[9] D.M. Stocco, B.J. Clark, Regulation of the acute production of steroids in steroidogenic cells, Endocr. Rev. 17 (1996) 221–244.
[10] D.M. Stocco, The role of StAR protein in steroidogenesis: challenges for the future, J. Endocrinol. 164 (2000) 247–253.
[11] W.L. Miller, Molecular biology of steroid hormone synthesis, Endocr. Rev. 9 (1988) 295–318.
[12] H.S. Bose, T.J.F. Sugawara 3rd., W.L. Strauss Miller, The pathophysiology and genetics of congenital lipoid adrenal hyperplasia, N. Engl. J. Med. 335 (1996) 1870–1878.
[13] K.M. Caron, S.C. Soo, W.C. Wetsel, D.M. Stocco, B.J. Clark, K.L. Parker, Targeted disruption of the mouse gene encoding steroidogenic acute regulatory protein provides insights into congenital lipoid adrenal hyperplasia, Proc. Natl. Acad. Sci. USA 94 (1997) 11540–11545.
[14] U.K. Laemmli, Cleavage of structural proteins during the assembly of the head of bacteriophage T4, Nature 227 (1970) 680–685.
[15] M.M. Bradford, A rapid and sensitive method for the quantification of microgram quantities of protein utilizing the principal of protein–dye binding, Anat. Biochem. 72 (1976) 248–254.
[16] P.J. Havel, Dietary fructose: implications for dysregulation of energy homeostasis and lipid/carbohydrate metabolism, Nutr. Rev. 63 (2005) 133–157.
[17] K.L. Stanhope, J.M. Schwarz, N.L. Keim, S.C. Griffen, A.A. Bremer, J.L. Graham, B. Hatcher, C.L. Cox, A. Dyachenko, W. Zhang, J.P. McGahan, A. Seibert, R.M. Krauss, S. Chiu, E.J. Schaefer, M. Ai, S. Otokozawa, k. Nakajima, T. Nakano, C. Beysen, M.K. Hellerstein, L. Berglund, P.J. Havel, Consuming fructose-sweetened, not glucose-sweetened, beverages increases visceral adiposity and lipids and decreases insulin sensitivity in overweight/obese humans, J. Clin. Invest. 119 (2009) 1322–1334.
[18] N. Semiane, F. Foufelle, P. Ferré, I. Hainault, S. Ameddah, A. Mallek, A. Khalkhal, Y. Dahmani, High carbohydrate diet induces nonalcoholic steato-hepatitis (NASH) in a desert gerbil, C.R. Biologies 340 (2017) 25–36.
[19] M. Krebs, M. Roden, Nutrient-induced insulin resistance in human skeletal muscle, Curr. Med. Chem. 11 (2004) 901–908.
[20] G.M. Reaven, Pathophysiology of insulin resistance in human disease, Physiol. Rev. 75 (1995) 473–486.
[21] I.S. Hwang, H. Ho, B.B. Hoffman, G.M. Reaven, Fructose-induced insulin resistance and hypertension in rats, Hypertension 10 (1987) 512–516.
[22] M.F. Dallman, S.F. Akana, K.A. Scribner, M.J. Bradbury, C.D. Walker, A.M. Strack, C.S. Cascio, Stress, feedback and facilitation in the hypothalamus-pituitary-adrenal axis, J. Neuroendocrinol. 4 (1992) 517–526.
[23] D. Pignatelli, P. Pinto, M.E. Azevedo, M.M. Magalhaes, M.C. Magalhaes, Acute stress effects on the adrenal cortex in the rat. A biochemical and immunohistochemical study, Endocr. Res. 22 (1996) 445–451.
[24] T. Buchenauer, P. Behrendt, F.J. Bode, R. Horn, G. Brabant, M. Stephan, H. Nave, Diet-induced obesity alters behavior as well as serum levels of corticosterone in F344 rats, Physiol. Behav. 98 (2009) 563–569.
[25] D.S. Jessop, M.F. Dallman, D. Fleming, S.L. Lightman, Resistance to glucocorticoid feed-back in obesity, J. Clin. Endocrinol. Metab. 86 (2001) 4109–4114.
[26] E.D. Kanter, C.W. Wilkinson, A.D. Radant, E.C. Petrie, D.J. Dobie, M.E. McFall, E.R. Peskind, M.A. Raskind, Glucocorticoid feedback sensitivity and adrenocortical responsiveness in posttraumatic stress disorder, Biol. Psychiatry. 50 (2001) 238–245.
[27] I. Sarel, E.P. Widmaier, Stimulation of steroidogenesis in cultured rat adrenocortical cells by unsaturated fatty acids, Am. J. Physiol. 268 (1995) 1484–1490.
[28] M. Ehrhart-Bornstein, V. Lamounier-Zepter, A. Schraven, J. Langenbach, H.S. Willenberg, A. Barthel, H. Hauner, S.M. McCann, W.A. Scherbaum, S.R. Bornstein, Human adipocytes secrete mineralocorticoid-releasing factors, Proc. Natl. Acad. Sci. USA 100 (2003) 14211–14216.
[29] L. Engström, K. Rosén, A. Angel, A. Fyrberg, L. Mackerlova, J.P. Konsman, D. Engblom, A. Blomqvist, Systemic immune challenge activates an intrinsically regulated local inflammatory circuit in the adrenal gland, Endocrinology 149 (2008) 1436–1450.
[30] P.W. Harvey, C. Sutcliffe, Adrenocortical hypertrophy: establishing cause and toxicological significance, J. Appl. Toxicol. 30 (2010) 617–626.
[31] M.M. Swierczynska, I. Mateska, M. Peitzsch, S.R. Bornstein, T. Chavakis, G. Eisenhofer, V. Lamounier-Zepter, S. Eaton, Changes in morphology and function of adrenal cortex in mice fed a high-fat diet, Int. J. Obes. (Lond.) 39 (2015) 321–330.
[32] G. Aguilera, A. Kiss, A. Lu, C. Camacho, Regulation of adrenal steroidogenesis during chronic stress, Endocr. Res. 22 (1996) 433–443.
[33] G.G. Nussdorfer, Cytophysiology of the adrenal cortex, Int. Rev. Cytol. 98 (1986) 1–405.
[34] J. Pudney, G.M. Price, B.J. Whitehouse, G.P. Vinson, Effects of chronic ACTH stimulation on the morphology of the rat adrenal cortex, Anat. Rec. 210 (1984) 603–615.
[35] S. Sricharoenvej, S. Boonprasop, P. Lanlua, S. Piyawinijwong, A. Niyomchan, Morphological and microvascular changes of the adrenal glands in streptozotocin-induced long-term diabetic rats, Ital. J. Anat. Embryol. 114 (2009) 1–10.
[36] W. Kanczkowski, A. Chatzigeorgiou, S. Grossklaus, D. Sprott, S.R. Bornstein, T. Chavakis, Role of the endothelial-derived endogenous anti-inflammatory

factor Del-1 in inflammation-mediated adrenal gland dysfunction, Endocrinology 154 (2013) 1181–1189.

[37] A. Stachowiak, G.G. Nussdorfer, L.K. Malendowicz, Proliferation and distribution of adrenocortical cells in the gland of ACTH- or dexamethasone-treated rats, Histol. Histopathol. 5 (1990) 25–29.

[38] N. Omari, Y. Aït-akli, F. Labrousse, M. Delage-Corre, M.J. Le Boutet, F. Hadj-Bekkouche, Stress nutritionnel chez Psammomys obesus : physiopathologie de la glande surrénale, Bull. Soc. Zool. Fr. 132 (2007) 163–181.

[39] T.J. Rosol, J.T. Yarrington, J. Latendresse, C.C. Capen, Adrenal gland: structure, function, and mechanisms of toxicity, Toxicol. Pathol. 29 (2001) 41–48.

[40] I.E. Tóth, D. Szabö, G.G. Bruckner, Lipoproteins, lipid droplets, lysosomes, and adrenocortical steroid hormone synthesis: morphological studies, Microsc. Res. Tech. 36 (1997) 480–492.

[41] G.G. Nussdorfer, G. Mazzocchi, V. Meneghelli, Cytophysiology of the adrenal zona fasciculate, Int. Rev. Cytol. 55 (1978) 291–365.

[42] H.L. Moses, W.W. Davis, A.S. Rosenthal, L.D. Garren, Adrenal cholesterol: localization by electron-microscope autoradiography, Science 163 (1969) 1203–1205.

[43] R. Singh, S. Kaushik, Y. Wang, Y. Xiang, I. Novak, M. Komatsu, K. Tanaka, A.M. Cuervo, M.J. Czaja, Autophagy regulates lipid metabolism, Nature 458 (2009) 1131–1135.

[44] H. Dong, M.J. Czaja, Regulation of lipid droplets by autophagy, Trends. Endocrinol. Metab. 22 (2011) 234–240.

[45] J. Müller, U. Pfeifer, J. Dämmrich, Inhibited autophagic degradation during ACTH-stimulated growth of rat adrenal zona fasciculata, Virchows. Arch. B. Cell. Pathol. 52 (1987) 429–441.

[46] S.A. Detmer, D.C. Chan, Functions and dysfunctions of mitochondrial dynamics, Nat. Rev. Mol. Cell. Biol. 8 (2007) 870–879.

[47] M.P. Valdecantos, P. Pérez-Matute, P. González-Muniesa, P.L. Prieto-Hontoria, M.J. Moreno-Aliaga, J.A. Martínez, Lipoic acid administration prevents nonalcoholic steatosis linked to long-term high-fat feeding by modulating mitochondrial function, J. Nutr. Biochem. 23 (2012) 1676–1684.

[48] M. Flamment, M. Arvier, Y. Gallois, G. Simard, Y. Malthièry, P. Ritz, P.H. Ducluzeau, Fatty liver and insulin resistance in obese Zucker rats: no role for mitochondrial dysfunction, Biochimie 90 (2008) 1407–1413.

[49] A. Nadal-Casellas, E. Amengual-Cladera, A.M. Proenza, I. Lladó, M. Gianotti, Long-term high-fat-diet feeding impairs mitochondrial biogenesis in liver of male and female rats, Cell. Physiol. Biochem. 26 (2010) 291–302.

[50] E. Kathirvel, K. Morgan, S.W. French, T.R. Morgan, Acetyl-carnitine and lipoic acid improve mitochondrial abnormalities and serum levels of liver enzymes in a mouse model of nonalcoholic fatty liver disease, Nutr. Res. 33 (2013) 932–941.

[51] H.C. Lee, Y.H. Wei, Mitochondrial biogenesis and mitochondrial DNA maintenance of mammalian cells under oxidative stress, Int. J. Biochem. Cell. Biol. 37 (2005) 822–834.

[52] A. Navarro, A. Boveris, The mitochondrial energy transduction system and the aging process, Am. J. Physiol. Cell. Physiol. 292 (2007) 670–686.

[53] M. Fukui, T. Nakamura, I. Ebihara, I. Shirato, Y. Tomino, H. Koide, ECM gene expression and its modulation by insulin in diabetic rats, Diabetes 41 (1992) 1520–1527.

[54] M. Reichenstein, R. Reich, J.G. LeHoux, I. Hanukoglu, ACTH induces TIMP-1 expression and inhibits collagenase in adrenal cortex cells, Mol. Cell. Endocrinol. 215 (2004) 109–114.

[55] M. Bosse, J. Chakir, M. Rouabhia, L. Boulet, M. Audette, M. Laviolette, Serum matrix metalloproteinase-9: tissue inhibitor of metalloproteinase-1 ratio correlates with steroid responsiveness in moderate to severe asthma, Am. J. Respir. Crit. Care Med. 159 (1999) 596–602.

[56] Y. Tomita, M. Nihira, Y. Ohno, S. Sato, Ultrastructural changes during in situ early postmortem autolysis in kidney, pancreas, liver, heart and skeletal muscle of rats, Leg. Med. (Tokyo) 6 (2004) 25–31.